



Desalination 107 (1996) 171-193

# Solving equations simulating the steady-state behavior of the multi-stage flash desalination process

Hisham El-Dessoukya\*, S. Bingulacb

<sup>a</sup>Department of Chemical Engineering, <sup>b</sup>Electrical and Computer Engineering Department Kuwait University, PO Box 5969, 13060 Safat, Kuwait Tel. 481-7662; Fax 483-9498; 481-7451

Received 12 January 1996; accepted 1 April 1996

#### Abstract

The paper presents an algorithm for solving the equations simulating the steady-state behavior of the multi-stage flash (MSF) desalination process. The model can be used either for designing new plants or anlysis and optimization of existing units. The set of equations relating the large number of design and operating variables for any stage (i-th stage) in MSF plants is broken down into three subsets. The first subset contains equations describing processes in the tubes of the preheater inside the flashing chamber. The second subset deals with the processes inside the flashing chamber. These two subsets of equations are subsequently solved iteratively involving only a single variable for each subset. These variables are: (1) saturation temperature  $T_{vi}$  of the flashed-off vapor and (2) temperature of the unevaporated brine flowing from the chamber. The third subset of equations considers the existing interactions between the first two subsets. This subset defines the mass of vapor formed by flashing  $D_i$  in the i-th stage. All equations in the above-mentioned subsets are solved by a reliable and efficient one-dimensional fixed-point iteration. The main advantages of this method are less sensitivity to initial guesses, fewer iterations to obtain the required solution, and no need for calculating derivatives. The algorithm is implemented using the computer-aided design (CAD) interative package L-A-S (Linear Algebra and Systems). Detailed results are presented to show the dependence of the important factors controlling the fresh water cost, which are plant performance ratio, specific heat transfer area, specific brine flow rate, and specific cooling water flow rate, on the most significant two design variables, namely the total number of stages and the top brine temperature. The predicted data from the model are compared with published data of a typical MSF plant in operation at Kuwait. The agreement was found to be very good.

Keywords: MSF desalination process; Modelling and simulation of MSF plants; Stage-by-stage algorithm; non-linear equations; Computational algorithm

#### 1. Introduction

All life on earth depends on fresh water. Unfortunately fresh water, like most other natural resources, is unevenly distributed in the universe. In January–February 1995, flooding in many places in Europe caused a lot of damage and the loss of huge amounts of money. Hundreds of thousands of people were evacuated from their homes in the Netherlands. At the same time many countries in the Middle East and North Africa spend an enormous amount of money to desalinate seawater.

In the last four decades large numbers of desalination plants have been installed in the Arabian Gulf countries. Most of these plants are multi-stage flash (MSF) units. Fig. 1 diagrammatically shows the MSF with brine recirculation desalination process. A lot of efforts have been made to reduce the cost of water produced from MSF plants. This has been achieved through the increase of plant capacity, improving the thermal performance of plants, better selection for construction materials, and good practice of reliable operation and scale control. These developments are a consequence of better understanding and good modeling and simulation of the MSF process.

Fig. 2 illustrates the interactions between different variables in stage number i in the heat recovery section. There are many models developed to find a functional relationship between the MSF process design variables and the different operating parameters [1-10]. The models are well developed from the basic laws of total and component mass balances, enthalpy balance coupled with heat and mass flow rate coefficients. These models must be supported by equations for calculating the thermal and physical properties of fresh and salt waters as functions of temperature and salinity. These models are either simplified or very complicated. The simplified models are based on many assumptions such as a constant temperature drop for each stage, a constant specific heat at constant pressure for

water with different salt concentrations and at different boiling temperatures, neglecting the thermal losses between the plant and its surroundings, constant heat transfer coefficient in the three different sections of the plant, and no thermodynamic losses inside the flashing chambers. These assumptions cause a larger discrepancy in the result of the models and the actual data.

A very limited number of publications considered the effect of thermodynamic losses on the plant thermal performance ratio. Silver [7], for the first time, showed the dependence of the performance ratio of MSF plants on the basic parameters and the thermodynamic losses to a very good approximation. El-Dessouky [8] developed a mathematical model which relates the most important factors affecting the fresh water cost, namely the plant thermal performance and the specific heat transfer area to the main design and operating parameters taking into consideration the effect of the different thermal losses.

Helal et al. [5] and Khan [3] considered the thermal losses in their mathematical models. Their models are based on a constant heat transfer area in each stage of the MSF plant. In these models the equations describing the process are numerous, non-linear and complex. Khan described the method of solving these equations by stage-to-stage calculations. Helal et al. [5] used the data from previous literature to linearize the balance and heat transfer relations. They used a special algorithm to solve these equations simultaneously. Their method is numerically stable and convergence is rapidly approached over a wide range of initial conditions.

Husain et al. [9] reported that the following points should be considered for enhancing the agreement of the steady-state model with the actual plant data: heat losses from the individual stages plus brine heater, vapor leak to ejector system, presence of air and other noncondensable gases and evaporation from the product tray. Although many investigators have

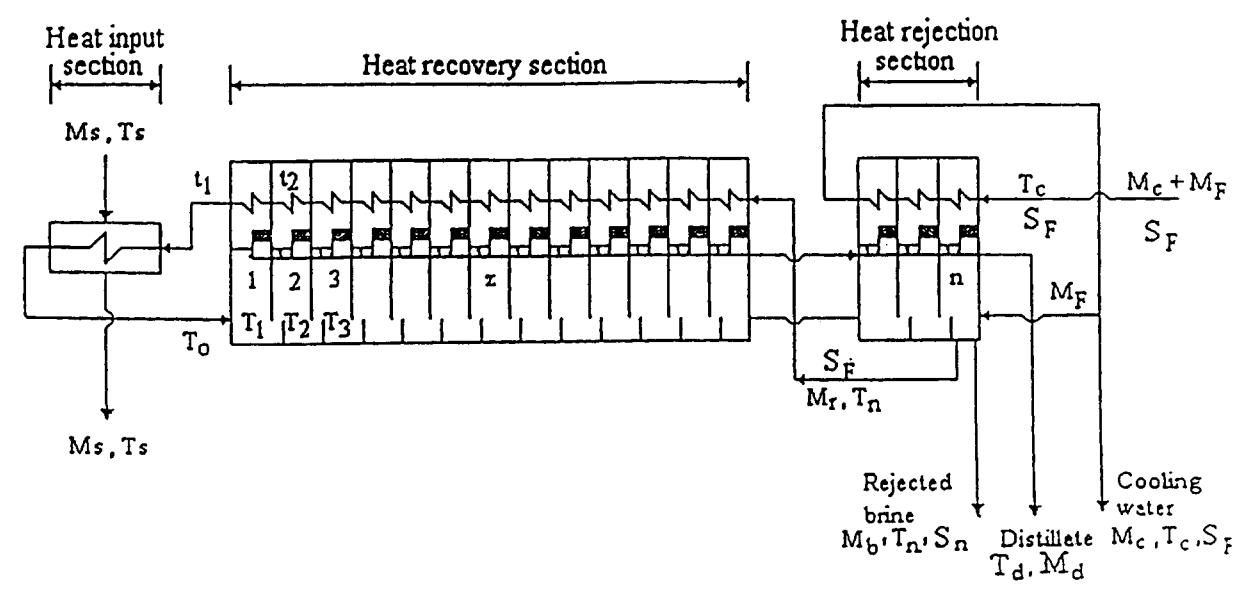


Fig. 1. Multi-stage flash desalination process.

modeled or analyzed the MSF desalination process, a detailed evaluation of the influence of the all variables on the process parameters has not been reported in the literature.

El-Dessouky et al. [1] developed a detailed steady-state mathematical model for the MSF desalination process. The main features of this model are:

- The basic assumption in the model is the practice case of constant heat transfer area in each section of the plant. In practice it is not economical to design MSF plants to have uniform interstage temperature differences over the entire flash range. It is therefore usual to design and construct all of the stages in each section with identical heat transfer surfaces.
- It considered the effect of the heat losses from the stages and the brine heaters to the surroundings and the vapor leak to the ejector system on the thermal performance of the process.
- It contemplated the variation in the stage flash down and thermodynamic losses (non-equilibrium allowance, boiling point elevation, temperature depression correspond-

ing to pressure drop in the demister and the condenser) from stage to stage.

- It studied the effect of flashing temperature, velocity of brine flowing through the tubes of brine heater and preheaters, the tube material of construction, flashing chamber geometry on plant performance ratio and the required specific heat transfer surface area.
- It takes into consideration the effect of temperature and salinity on the water physical properties such as density, dynamic viscosity, specific heat at constant pressure and Prandtle number.
- It discusses the effect of presence of air and non-condensable gases and the extent of fouling on the design of the process.

There are some software packages which are suitable for designing or rating the MSF desalination process. However, these packages are not available for many engineers in the field. Also, the model on which these packages were built and the assumptions involved are not presented in the literature.

The main purpose of this paper is to present an algorithm for solving the equations describing the

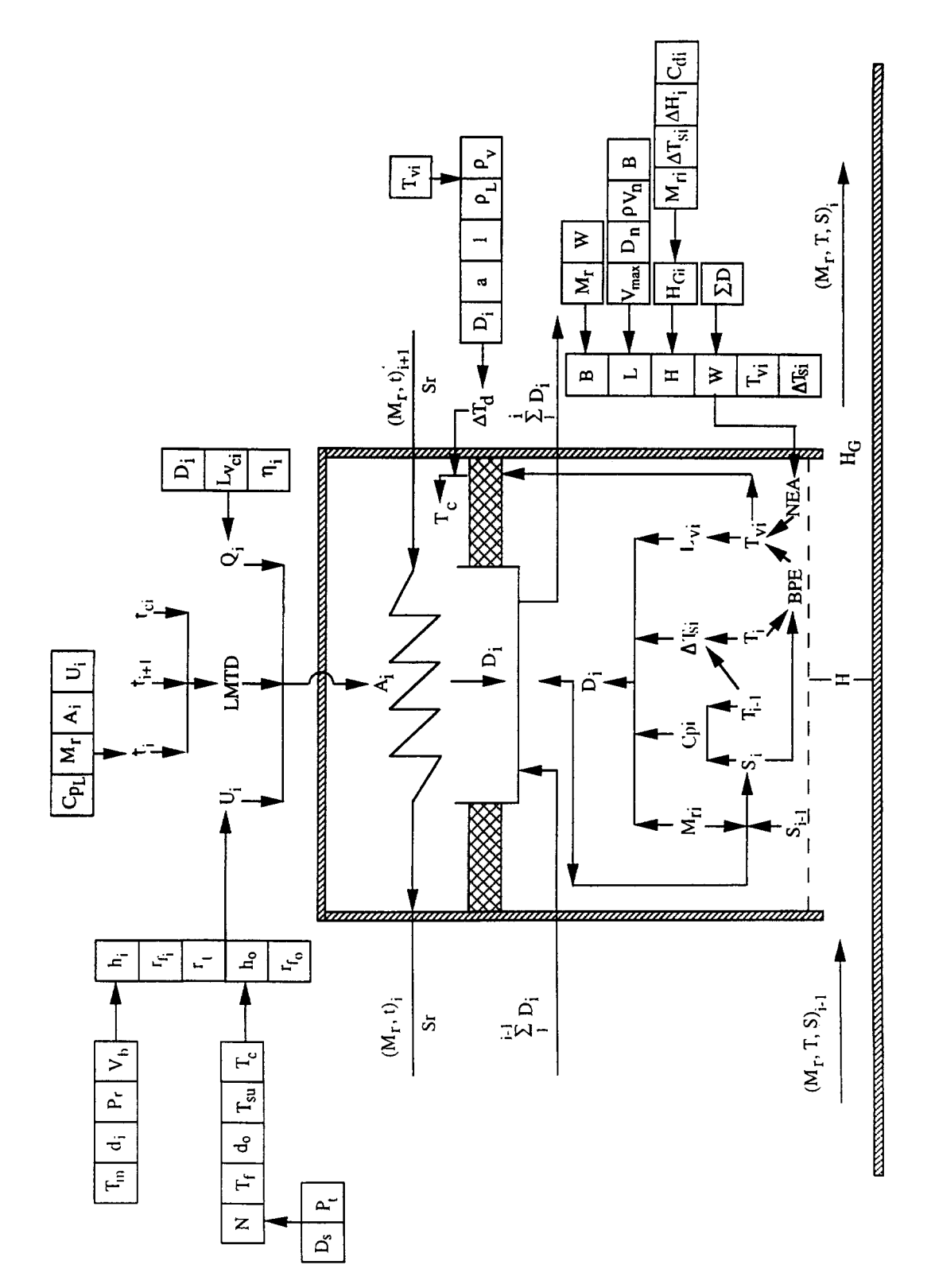


Fig. 2. Interaction between different variables in MSF flashing chamber.P

steady-state behavior of the MSF desalination process as developed by El-Dessouky et al. [1]. Also, the algorithm is an attempt to bridge the gap between the classical analysis and the commercial software packages.

# 2. Structure of the algorithm

In considering an algorithm for solving a model describing the steady-state behavior of MSF plants — consisting of a set of highly nonlinear equations — it was not advisable to use any numerical procedure requiring linearization and/or differentiation as, for instance, the well known and convergent procedures as Newton-Raphson, TDM and the like. It was necessary to resort to simple, but yet powerful and convergent procedures as a secant method and the fixed point iteration [11]. To this end, the complete model of the MSF plant has been first divided into three parts: heat recovery section, heat rejection section, and the brine heater.

Next, all equations describing the processes in the heat recovery and heat rejection sections were grouped according to stages, and then the well known relations between variables in successive stages were established. Finally, equations describing a single stage (either the recovery or rejection stage) were divided into the following three groups: brine flowing through the brine preheater, non-evaporating brine flowing through the flashing chamber, and mass of vapor formed.

By analyzing these groups of equations individually, it was concluded that it is possible to express formally each group of these equations as a single nonlinear equation with only one variable, as shown in Appendix 2.

The most important characteristics of the proposed algorithm are:

 Decomposition of all non-linear equations describing behavior of the i-th stage of an MSF plant into three subsets of equations where each subset is represented by a single non-linear equation with only one independent variable

- The use of reliable convergent iterative procedures involving only one independent variable, which considerably simplifies computational aspect of the procedure
- Flexibility in changing any design value, constant or geometrical parameter, which considerably facilitates analysis and optimization of MSF plants
- Taking into account a large number of effects existing in MSF plants, thus making the results of simulation sufficiently close to the behavior of real processes.

# 3. Modifications of the fixed point iteration scheme

It is well known [12] that the classical fixed point iterative scheme, defined by

$$x_{i+1} = g_k(x_i, q), \quad i = 0, 1, ...$$
 (1)

suffers from the limitation that it diverges when the first derivative  $g_k(x,q)|_{x,p}$  of the function  $g_k(x,q)$  in the vicinity of the fixed point x=p satisfies

$$|g_k(p,q)| > 1 \tag{2}$$

In order to achieve convergence regardless of the value of the first derivative  $g_k(x,q)$  in the vicinity of the fixed point, the following modification is used:

$$x_{i+1} = [g_k(x_i,q) + x_i(\alpha-1)]/\alpha; \quad i=1,1,2,...$$
 (3)

where  $\alpha$  is an arbitrary, non-zero-free parameter. It may be easily verified that both schemes (2) and (4) have the same fixed point, x=p, i.e., for

$$x_{i+1} = x_i = p = g_k(x_i, q)$$

both the equations are satisfied for any non-zero value of  $\alpha$ . It should be noted that for  $\alpha=1$ , Eq. (3) reduced to (1).

The free parameter  $\alpha$  in the modified algor-

ithm (3) should be calculated as

$$\alpha = 1 - [g_k(x_{i}, q) - g_k(x_{i-1}), q] / (x_i - x_{i-1})$$
(4)

It may be shown that if the stabilizing quantity  $\alpha$  is calculated according to (4), the algorithm (3) behaves similarly as the Secant method. Note that it is not necessary to calculate the quantity  $\alpha$  in each iteration.

# 4. Computational algorithm

MSF desalination plants as shown in Fig. 1 consist of three different sections: the heat recovery section, heat rejection section, and heat input section. Equations describing each section are given in Appendix 1.

The algorithm for the first part, the heat recovery section, is represented in more detail in Fig. 3. Due to space limitation and since the equations for the heat rejection section are rather similar to those of the heat recovery section, the detailed algorithm for the second part is not shown. Similarly, since the equations for the brine heater are quite simple, not involving any iteration, the detailed algorithm for this part is also not shown.

Fig. 3 shows that the algorithm for solving the equations describing the heat recovery section consists of five loops. By loop #4 the sequential stage-by-stage calculation is performed. In other loops only one variable is adjusted at a time. These variables are:

Loop # 1 — Temperature  $T_{\nu i}$ , of the formed vapor in the *i*-th stage

Loop #2 — Temperature  $T_i$ , of non-evaporating brine flowing from the *i*-th stage

Loop # 3 — Distillate  $D_i$ , produced in the *i*-th stage

Loop #5 — Temperature  $t_i$ , outlet temperature of the brine flowing from the preheater tubes in the *i*-th stage)

As may be concluded from the equations describing processes in the *i*-th stage of the brine

preheater, referred to as Algorithm 1 (Appendix 2) and solved by loop # 1, the  $T_{vi}$  depends on both  $T_i$  and controlling  $D_i$  as well as  $t_{i-1}$ , which are calculated subsequently by loops #2, #3 and #5. Therefore, in order to initiate the calculation in loop #1 corresponding to the first stage, in addition to the design values  $\{T_0, A, N_1\}$ , also the initial guesses for the variables  $\{T_i, D_i\}$ , i.e.,  $\{T_1, D_1\}$ , as well  $t_0$  should be provided. According to our experience, this does not represent a serious problem since basic relations between these temperatures are

$$T_{i-1} > T_i > T_{vi} > t_{i-1} > t_i \tag{5}$$

Thus, it is relatively easy to select satisfactory initial guesses for temperatures  $T_i$  and  $T_{vi}$  { $T_1$  and  $T_{vi}$ }, once the values temperatures  $T_{i-1}$  and  $t_{i-1}$  { $T_0$  and  $t_0$ } are given/chosen. Similarly, the initial guess for the value  $D_i$ , i.e.,  $D_1$ , may be conveniently selected from the basic knowledge of equations describing the MSF process and taking into account the used design values, particularly the values of A and  $N_1$ .

Once the calculations in loop #1 are completed, i.e., temperature  $T_{vl}$ , satisfying

$$T_{v1} = g_1(T_{v1}, T_1, D_1, q_1)$$
 (6)

is determined (for the given initial values of  $T_1$  and  $D_1$ ), the calculation in loop #2 starts. Note that simultaneously with  $T_{\nu 1}$ , temperature  $t_2$ , inlet temperature of the brine flowing inside the tubes of the preheater of the first stage, is also calculated. Within loop #2 the same initial value for  $D_1$  is used, while the value of  $T_{\nu 1}$  corresponds to the value obtained in loop #1. After several iterations, usually 3-5, the value of  $T_1$  is calculated when satisfying this requirement.

$$T_1 = g_2(T_{\nu 1}, T_0, T_1, D_1, q_2) \tag{7}$$

In both loops #1 and #2 for the value of the stabilizing factor  $\alpha_T$ , the quantity  $\alpha_T$ =1.1 is used.

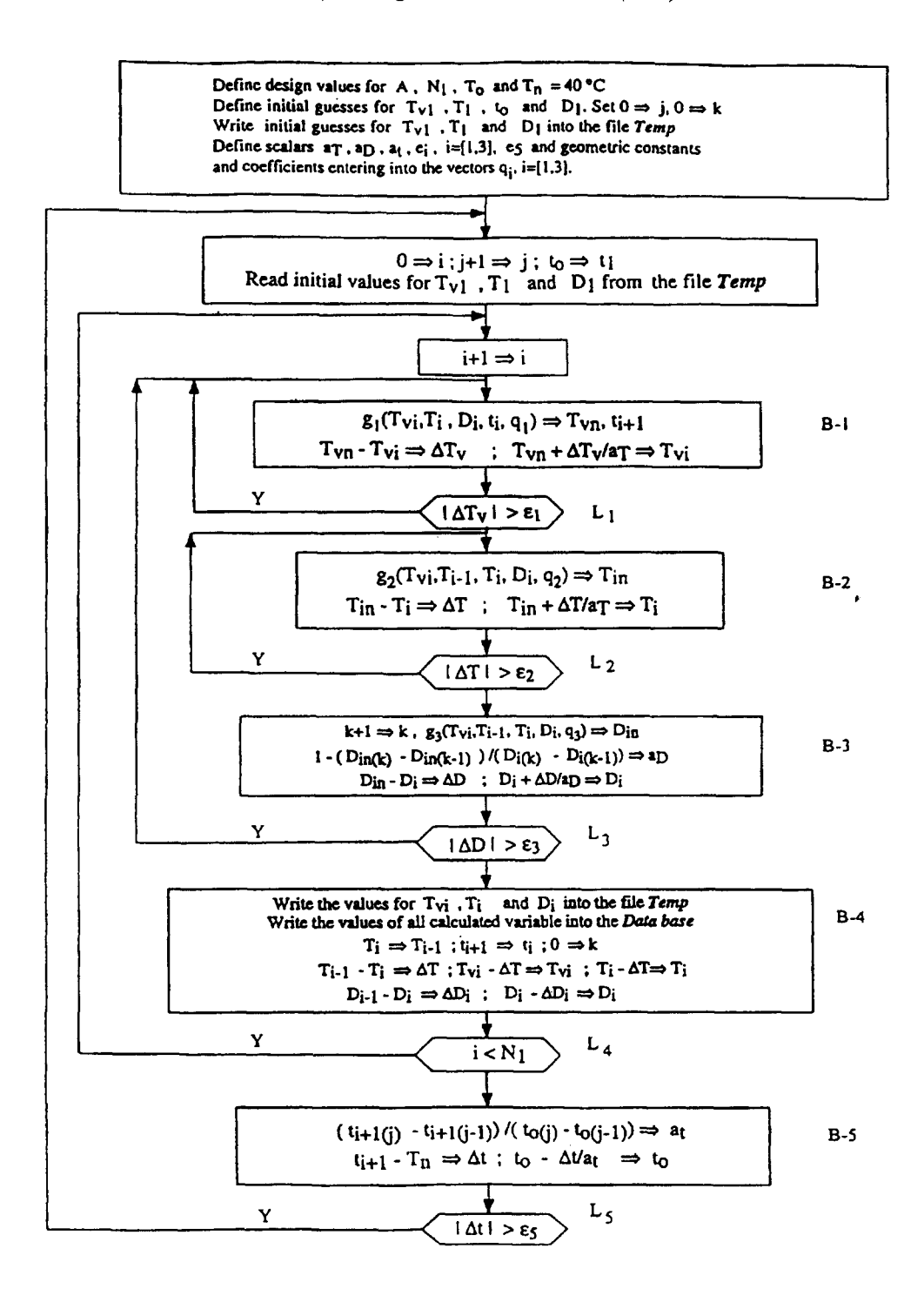


Fig. 3. Computational algorithm for stage number i in heat recovery section.

It has been verified experimentally that this value assures satisfactory convergence of the fixed point iterations in both loops and for all operating conditions. Quantities  $\varepsilon_1$  and  $\varepsilon_2$  in the first two loops are assumed to have the same value of  $\varepsilon_1$ =  $\varepsilon_2$ =10<sup>-5</sup>.

After the calculations in loop #2 are completed, the value of  $D_1$  is updated using the equations listed in Algorithm 3, with the above calculated values for  $T_{v1}$  and  $T_1$ . As is indicated in Fig. 3, the fixed point iteration has also been used. Here, however, the most convenient value of the stabilizing quantity  $\alpha_D$  depends on the operating conditions used. Therefore, as has been shown in Eq. (5) and indicated in Fig. 3, the new value for  $D_1$  by which calculations in loops #1 and #2 are repeated is updated by  $\Delta D/\alpha_D$ , i.e.:

$$D_1 + \Delta D / \alpha_D \Longrightarrow D_1$$

where the increment  $\Delta D/\alpha_D$  in the *first passage*, i.e., for k=1, is given by:  $D_1/50$ , while for the values of the iteration counter k > 1, shown in Fig. 3, the algorithm uses  $\Delta D/\alpha_D$  where

$$\Delta D = D_{\text{in}(k)} - D_{i(k)}, \quad \text{and}$$
 (8)

$$\alpha D = \left\{ 1 - \left( D_{\text{in}(k)} - D_{\text{in}(k-1)} \right) \right\} / \left( D_{i(k)} - D_{i(k-1)} \right) \quad (9)$$

Depending on the used operating condition, the value of the quantity  $\alpha_D$  varies between 2–6. Since the absolute value of  $D_i$  is relatively small, of the order of magnitude of  $10^{-1}$ , for the quantity  $\epsilon_3$  in loop #3, the value of  $\epsilon_3 = 10^{-7}$  is used. As has been mentioned previously, calculations in loops 1, 2 and 3 are now repeated using new, updated values of  $D_1$ . Due to the stabilization of the fixed point iteration procedure by which the value of  $D_1$  is updated, after several iterations, usually 3 through 5,  $\Delta D = D_{\text{in}(k)} - D_{i(k)}$  satisfies the condition

$$|\Delta D| < \varepsilon_3$$
 (10)

At this point all equations (Algorithms 1, 2 and 3 in Appendix 2) corresponding to the first stage, i=1, of the recovery section are solved.

In order to start calculations for the second stage, i.e., for i=2, appropriate initial values for  $T_{v2}$ ,  $T_2$  and  $D_2$  should again be selected. This is done in the block B-4 shown in Fig. 3. Note that in this block the value of the iteration counter k is reset to zero. Also the values of large numbers of variables mentioned above are written in the data base. In addition to that values of variables  $\{T_{vi}, T_i, D_i\}$  are written to the temporary file Temp. The use of the file Temp will be explained later. After calculations corresponding to all  $N_1$  stages are completed, the algorithm exits from loop #4 and enters into block B-5, which is a part of loop #5.

Recall that in loop #1, in addition to the variable  $T_{vi}$ , the variable  $t_{i+1}$ , which is the inlet temperature of the brine flowing to the preheater tubes of the *i*-th stage, is also calculated. In the case of the last,  $N_1$ -th stage of the recovery section, this temperature corresponds to the temperature of the brine entering the preheater of the recovery section. It is well known that this temperature is a design variable and that its value is  $T_n=40$ °C. Therefore, in block B-5 of the algorithm, the temperature  $t_1$ , outlet temperature of the first stage, is updated so that the value  $t_{i+1}$  for  $i = N_i$ reaches the design value  $T_n$ . The updating of  $t_1$ , as shown in Fig. 3, is accomplished using the Secant method, which again does not require any differentiation of nonlinear equations to be solved. The factor at, which assures convergence of the updating of  $t_1$ , is calculated as shown in Fig. 3. The initial value of the factor  $\alpha_n$ , i.e., for j=1, is selected to be  $\alpha$ =5, which works satisfactorily for all used operating conditions.

After updating the value  $t_1$ , as shown in Fig. 3, the calculations return back to loop #1, corresponding to the first stage, i.e., for i=1. The only, but important, difference is that the required initial values for variables  $\{T_{\nu_1}, T_1, D_1\}$  are now read from the file Temp, which guarantees

convergence and considerably reduces the number of iterations in loops 1, 2 and 3. Similarly, if required, the values of  $\{T_{vi}, T_i, D_i\}$  for i > 1, could be read from the file Temp, instead of defining them as indicated in block B-4 (Fig. 3). In fact, it is suggested to use this option for j > 3 since then, due to excellent convergence properties of the algorithm, the variations of values  $\{T_{vi}, T_i, D_i\}$  for successive values of the iteration counter j are relatively small.

Finally, after reaching the condition

$$|\Delta t| \le \varepsilon_5 \tag{11}$$

where  $\varepsilon_5=10^{-4}$  see loop # 5, Fig. 3, the solution of all equations describing the processes in the recovery section, corresponding to the used design values  $\{T_0, A, N_1\}$  is considered completed.

Then the similar calculations are performed using the equations describing the processes in the heat rejection section. These calculations are much more simple compared to those of the heat recovery section. In the heat rejection section only three stages are assumed, and all required initial guesses for the first stage of the rejection section are taken from the last stage of the heat recovery section.

Finally, having all temperature profiles satisfying the used design values for both recovery and rejection sections, equations corresponding to the brine heater are solved.

# 5. Application of the algorithm

The algorithm developed in the previous sections has been used to obtain basic relationships between the most important variables controlling the cost of water produced from an MSF desalination plant. These parameters are the number of flashing stages, top brine temperature, specific heat transfer area, specific recirculating brine flow rate, and the specific cooling water flow rate. The assumptions employed in generating these relationships are:

- The sum of the heat transfer resistances due to the tube material, fouling inside the tube, and fouling outside the tube is 731×10<sup>-6</sup> m<sup>2</sup>K/W.
- The thermal efficiency of the flashing chamber is 90%.
- The tubes used have an outside diameter of 31.75 mm and inside diameter of 19.75 mm.
- The velocity of brine flowing inside the tubes is 1.55 m/s.
- The temperature and the concentration of salt in the rejected brine from the last stage are constant and equal to 40°C and 70,000 ppm, respectively.
- The temperature and salt concentration in feed water are constant and equal to 30°C and 42,000 ppm.
- The number of stages in the heat rejection section is 3.
- The thickness of the demister is 100 mm.
- The temperature of steam condensing in the brine heater is always higher than the top brine temperature by 10°C.

The effects of both the number of stages and the top brine temperatures on the plant performance ratio, specific heat transfer surface area, specific recirculating brine flow rate, and the specific cooling water flow rate are shown in Figs. 4–7, respectively.

On the other hand, the algorithm is used to compare the data calculated from the developed model and the design conditions of a plant already in operation at Doha West, Kuwait. The basic process data of this plant is given in Table 1.

Fig. 8 illustrates the calculated and reported values for the percentage of distillate formed at each stage. This percentage of distillate is defined as the mass of vapor formed in the stage divided by the total plant distillate water production rate. The comparison between the calculated and reported temperature of the flashing brine and the temperature of brine flowing inside the brine preheaters as function of stage number are depicted in Figs. 9 and 10, respectively.

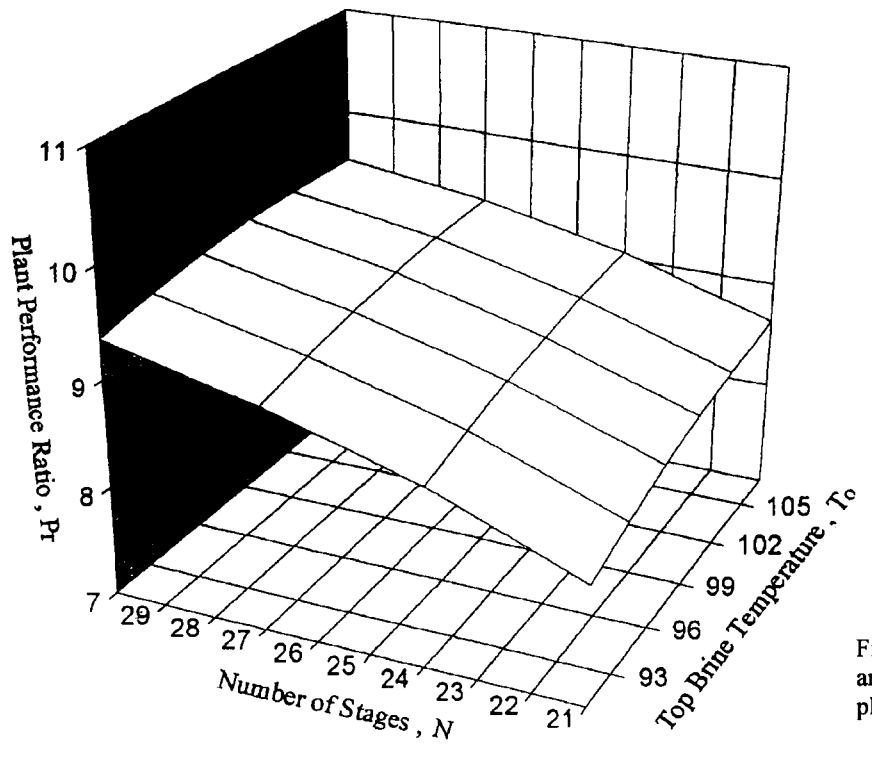


Fig. 4. Effect of number of stages and top brine temperature on the plant performance ratio.

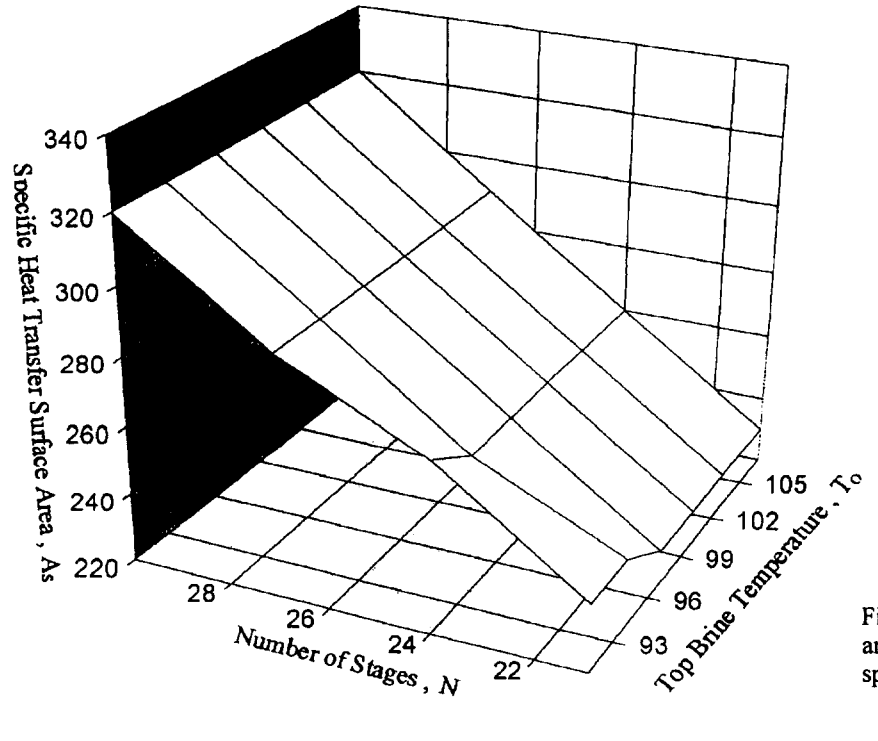


Fig. 5. Effect of number of stages and top brine temperature on the specific heat transfer surface area.

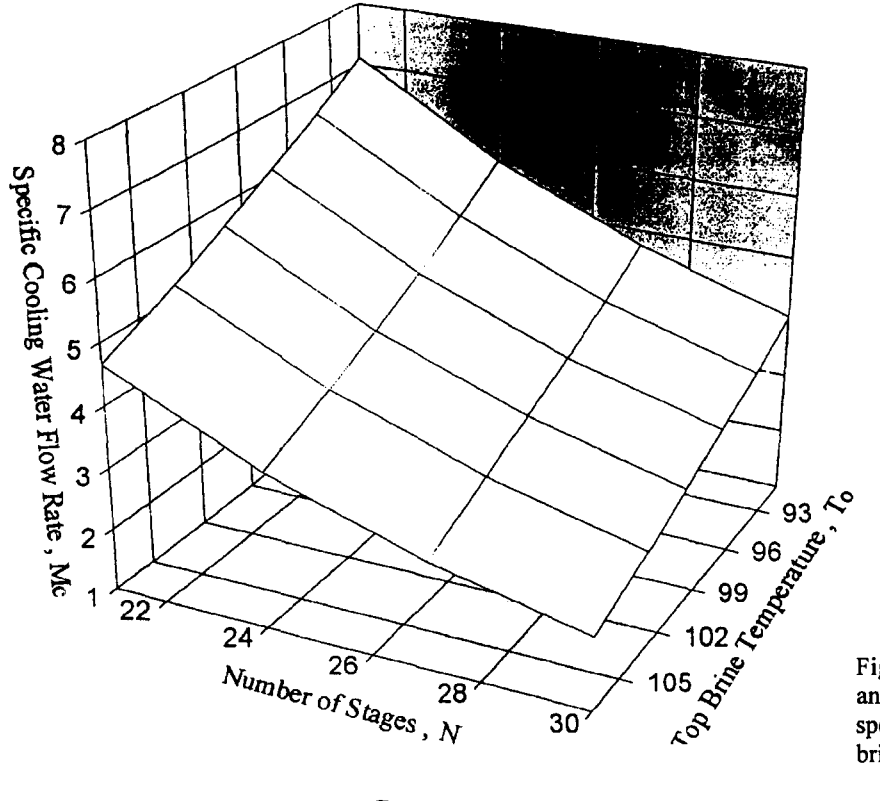


Fig. 6. Effect of number of stages and top brine temperature on the specific flow rate of recirculated brine.

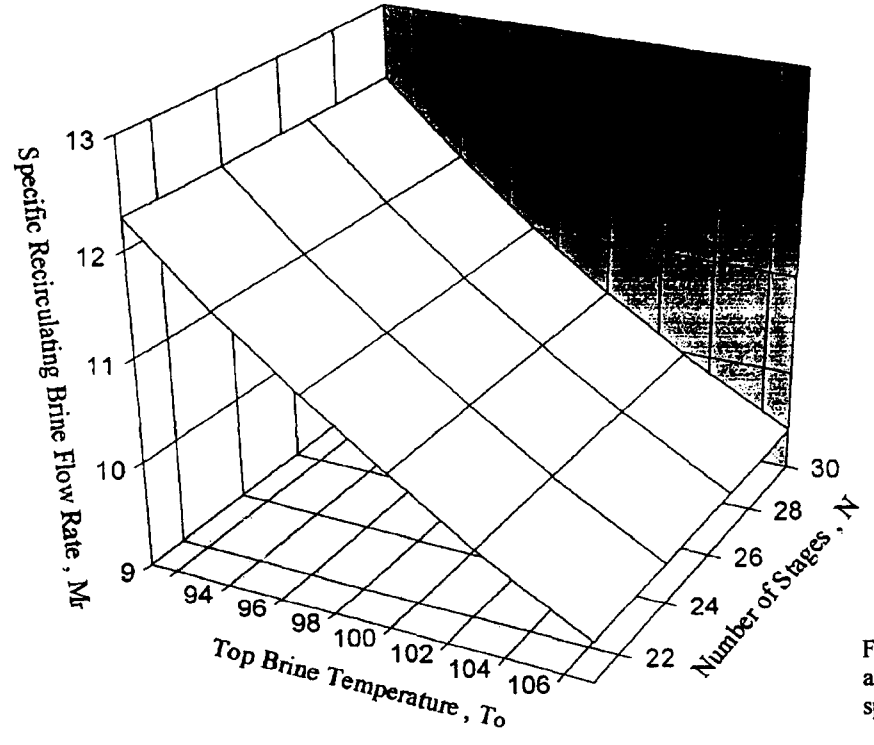


Fig. 7. Effect of number of stages an top brine temeprature on the specific flow rate of cooling water.

Table 1		
Data on a typical 6 migd	plant operating	at $T_0 = 90.54$ °C

Design parameter	Brine heater	Heat recovery stages		Heat rejection stages
		1st and 2nd stages	All other stages	
Clean heat transfer coefficient, kW/m <sup>2</sup> .C	4.57	3.58	4.92	4
Design heat transfer coefficient, kW/m <sup>2</sup> .C	2.07	2.33	2.83	2.25
Fouling factor (kW/m <sup>2</sup> .C)	.000263	.000149	.000149	.000194
LMTD	12.05	3.41	3.16	3.99
Brine velocity, m/s	2.13	1.98	1.98	2.08
Material	7/30 Cu-Ni	70/30 Cu-Ni	Al-brass	70/30 Cu-Ni
Area, m <sup>2</sup> /stage	3594	3676.5	3676	3148
Tube number in stage	1367	1451	1451	1588
Tube dimensions:				
OD, mm	43.8	43.8	43.8	3.42
Length, m	18.84	18.84	18.84	18.84

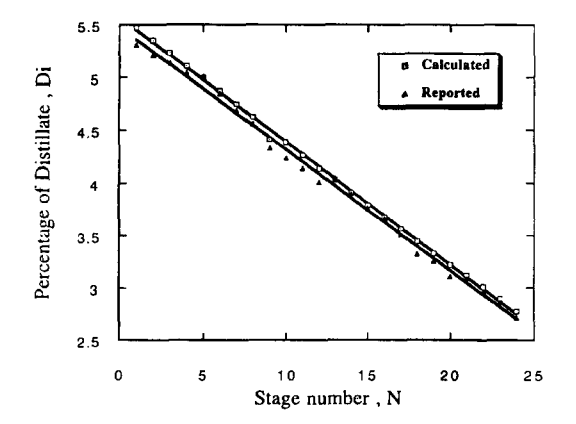


Fig. 8. Comparison of calculated and reported percentages of formed distillate.

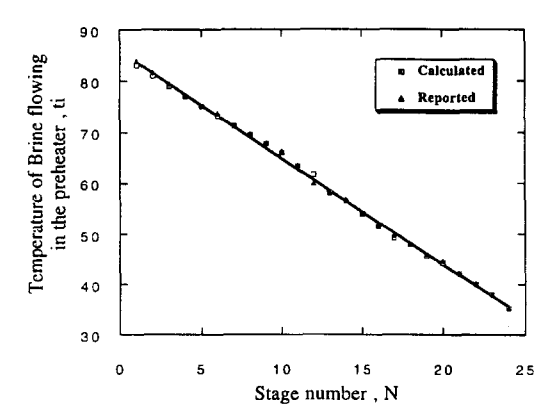


Fig. 10. Comparison of calculated and reported temperatures of brine flowing in the brine preheater.

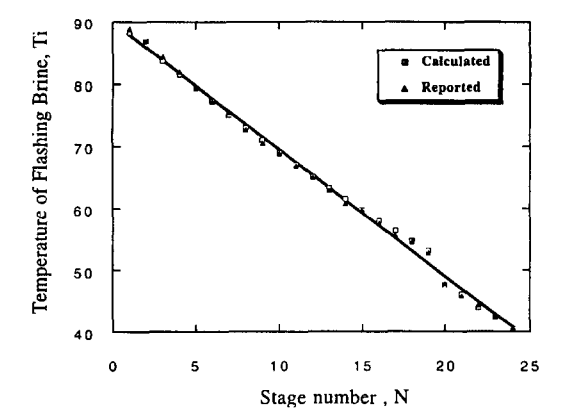


Fig. 9. Comparison of calculated and reported temperatures of flashing brine.

As can be seen from the last three figures, there is very good agreement between the calculated and reported design data.

#### 6. Conclusions

An algorithm for solving the huge number of equations describing the steady-state model of MSF desalination plant is presented. The developed algorithm belongs to the class of stage-by-stage approach and starts from the high temperature flashing chamber. The equations relating the different variables in each stage are broken down into three subsets. The equations in

the three subsets are solved by a reliable and efficient one-dimensional fixed-point iteration. The developed algorithm was implemented using the computer-aided design (CAD) interacitve package L-A-S. The effect of both the top brine temperature and the number of stages on the specific heat transfer area, specific brine recirculation flow rate, specific cooling water flow rate, and the plant performance ratio are presented. Good agreement was found between the data of a real plant already in operation and those obtained from the model.

# 7. Symbols

- a Demister cross sectional area, m<sup>2</sup>
- A Heat transfer area, m<sup>2</sup>
- A<sub>c</sub> Heat transfer surface area of the heat recovery section, m<sup>2</sup>
- A<sub>h</sub> Heat transfer surface area of the brine heater, m<sup>2</sup>
- A<sub>j</sub> Heat transfer surface area of the heat rejection section, m<sup>2</sup>
- B Width of flashing chamber, m
- BPE Boiling point elevation, K
- C<sub>p</sub> Specific heat at constant pressure of the flashing brine, kJ/Kg K
- C'<sub>p</sub> Specific heat at constant pressure of the brine flowing inside the preheaters tubes, kJ/kg.K
- C"<sub>p</sub> Specific heat at constant pressure of the distillate water, kJ/kg.K
- Mass of vapor formed by flashing, kg/s
- D<sub>s</sub> Shell diameter, dimensionless
- $d_i$  Tube inside diameter, m
- $d_a$  Tube outside diameter, m
- $g_{\nu}(x)$  Non-linear function of x
- H Height of brine in the flashing chamber, m
- H<sub>G</sub> Height of the gate in the flashing chamber, m

- h Heat transfer coefficient, W/m<sup>2</sup>. °K
- Number of stages in the heat rejection section, dimensionless
- K Thermal conductivity, W/mK
- Length of the flashing chamber, m
- $L_v$  Latent heat of evaporation, kJ/kg
- Thickness of the demister pad, m
- M Mass flow rate, kg/s
- Total number of flashing chambers, dimensionless
- Number of rows of horizontal tubes in the condenser, dimensionless
- N<sub>t</sub> Total number of tubes in the condenser, dimensionless
- Nu Nusselt number based on the surfaceaveraged heat transfer coefficient, dimensionless
- NTU Number of transfer units, dimensionless
- NEA Non-equilibrium allowance, K
- P Value of  $X_i$  (fixed point of  $g_k(x)$  satisfying  $P=g_k(x_{i,o})$
- Pv Saturation vapor pressure, Pa
- Pr Prandtl number, dimensionless
- P, Pitch
- q Vector containing design values
- Q Heat transfer rate, W
- R Universal gas constant, kJ/kg K
- Re Reynolds number, dimensionless
- r, Thermal resistance of the tube material, m<sup>2</sup>K/W
- Thermal resistance of the scale on the inside of the tubes, m<sup>2</sup>K/W
- r<sub>fp</sub> Thermal resistance of the scale on the outer surface of the tubes, m<sup>2</sup>K/W
- S Water salinity, ppm
- Temperature of the brine flashing in the stages, K
- $T_0$  Top brine temperature, K
- Temperature of brine flowing inside the preheaters tubes, K
- $T_c$  Condensation temperature, °K

 $T_{su}$  — Surface temperature

 $U_o$  — Overall heat transfer coefficient,  $W/m^2$ .  ${}^{\circ}K$ 

V — Velocity, m/s

v<sub>g</sub> — Specific volume of the saturated vapor, m<sup>3</sup>/kg

Xi — Unknown variable (Scalar)

W — Recirculated brine mass flow rate per unit length of chamber width, Kg/m.s

Z — Stage number in the heat rejection section

#### Greek

α — Stabilizing quantity

 $\Delta P$  — Pressure drop, N/m<sup>2</sup>

 $\Delta P_d$  — Pressure drop due to the vapor flow through the demister, N/m<sup>2</sup>

 $\Delta T$  — Temperature difference

 $\Delta T_d$  — Temperature decrease corresponding to the pressure drop in the demister,  ${}^{\circ}K$ 

 $\Delta T_s$  — Stage flashing range, °K

μ — Viscosity

δ — Density, Kg/m<sup>3</sup>

#### Subscripts

1,2,...n Stage number

b — Rejected brine

c — Cooling water

d — Product fresh water

f — Feed water

l — Liquid

r — Recirculated brine

s — Heating steam

v — Vapour

#### Acknowledgements

The research reported in this paper has been supported in part by the Research Administration, Kuwait University, under Project EE 058.

#### References

- H. El-Dessouky, H.I. Shaban and H. Al-Ramadan, Desalination, 103 (1995) 271.
- [2] A.H. Khan, Desalination Processes and Multi Stage Flash Distillation Practice. Elsevier, Amsterdam, 1986.
- [3] M.A. Darwish, Desalination, 85 (1991) 59.
- [4] A.M. Omar, Desalination, 45 (1983) 65.
- [5] A.M. Helal, M.S. Medani, M.A. Soliman and J.R. Flower, Computers and Chemical Engineering, 10(4) (1986) 327.
- [6] C.D. Hornburg and R.M. Watson, Desalination, 92 (1993) 333.
- [7] R.S. Silver, Multi-stage flash desalination, the first ten years. Proc., 3rd Internat. Symp. on Fresh Water from the Sea, Vol. 1, 1970.
- [8] H.T. El-Dessouky and G. Assassa, Losses in MSF desalination plants. Proc., 3rd Joint Conference on Mech. Eng. Technology, Cairo, 1985.
- [9] A. Hussain, A. Hassan, D.M. Al-Gobaisi, A. Al-Radif, A. Woldai and C. Sommariva, Desalination, 92 (1993) 21.
- [10] J.M. Montagna, N.J. Scenna and T. Melli, Desalination, 84 (1991) 437.
- [11] S. Bingulac and H.F. Van Landingham, Algorithms for Computer Aided Design of Multivariable Control Systems. Marcel Dekker, New York, 1993.
- [12] J. Mathews, Numerical Methods for Mathematics, Science and Engineering. Prentice Hall, Englewood Cliffs, N.J., 1992.

# Appendix 1

At steady-state operation, the mass of vapor formed by flashing in the first stage  $D_1$  is given by

$$D_1 = M_r C_{p1} \frac{T_0 - T_1}{L_{v1}}$$
 (A1.1)

The temperature of the unevaporated brine flowing to the second stage  $T_1$  is related to the saturation temperature of the formed vapor  $T_{\nu 1}$  by this equation:

$$T_1 = T_{v1} + BPE_1 + NEA_1 \tag{A1.2}$$

The following two correlations are used to calculate the NEA:

$$NEA_{10} = (0.9784)^{T_0} (15.7378)^H (1.3777)^{[w]10^{-6}}$$
(A1.3)

$$NEA = \left[\frac{NEA_{10}}{0.5DT_s + NEA_{10}}\right]^{0.3281L} \left[0.5DT_s + NEA_{10}\right]$$
(A1.4)

Eq. (3) is applicable only for a stage of 10 ft in length, while Eq. (4) is used for stages of any other lengths.

The brine flow rate per unit length of chamber width W is calculated from the following correlation which gives fairly typical values.

$$W = 105.6 + 18.06 M_d \tag{A1.5}$$

The chamber length is dictated by the vapor release rate at the brine surface. That is,

$$L_1 = \frac{D_1}{\delta v_1 V_m B} \tag{A1.6}$$

The chamber width B can be calculated from this simple relation.

$$B_1 = \frac{M_r}{W} \tag{A1.7}$$

The gate height HG can be calculated from the following equation:

$$HG = \frac{M_r}{C_d B} (2d\Delta P)^{1/2}$$
 (A1.8)

The pressure difference  $\Delta P$  between stage 1 and the adjacent 2 can be calculated from this equation:

$$\Delta P = P_{v1} - P_{v2} + \delta_L (H_1 - H_2) \tag{A1.9}$$

The following equation can be used to relate the pressure drop between the stages  $\Delta P_{\nu 1-2}$  to the vapor saturation temperatures in the stages.

$$\Delta P_{\nu 1-2} = P_{\nu 1} \left[ 1 - \exp \frac{L_{\nu 1}}{T_{\nu 1} R} \left( \frac{T_{\nu 1} - T_{\nu 2}}{T_{\nu 1} T_{\nu 2}} \right) \right]$$
(A1.10)

The boiling point elevation (BPE) depends on both the brine salinity S and the flashing temperature T. The BPE in  $^{\circ}$ K is given by

$$BPE = S(B+CS) (A1.11)$$

Both coefficients B and C are functions of T as follows:

$$B = [6.71 + 6.43 * 10^{-2}T + 9.74 * 10^{-5}T^{2}]10^{-3}$$
(A1.12)

$$C = [22.238 + 9.59 * 10^{-3}T + 9.42 * 10^{-5}T^{2}]10^{-5}$$
(A1.13)

The salinity of brine flowing from the first chamber to the second one  $S_1$  is related to the recirculated brine salinity  $S_0$  by the following

relationship:

$$S_1 = \frac{M_r S_0}{M_r - D_1} \tag{A1.14}$$

The frictional pressure drop due to the vapor flow inside the wire mesh mist eliminator is calculated from this formula:

$$\Delta P_d = 3.296 * 10^{-13} \ln \left( \frac{\delta_L}{\delta v} \right) \left( \frac{D}{a} \right)^2 \qquad (A1.15)$$

The vapor saturation temperature decrease  $(\Delta T_d)$  due to the pressure drop in the demister  $(\Delta P_d)$  can be calculated using the following formula:

$$\Delta T_d = \frac{T_{v1}^2 \left( R/L_{v1} \right) \ln \left[ P_{v1} / \left( P_{v1} - \Delta P_{d1} \right) \right]}{1 + T_{v1} \left( R/L_{v1} \right) \ln \left[ P_{v1} / \left( P_{v1} - \Delta P_{d1} \right) \right]} \quad (A1.16)$$

The rate of heat transfer between the vapor condensing outside the tubes and recirculated brine flowing inside the tubes of the preheater of the first stage can be written in terms of an overall heat transfer coefficient  $U_1$ , preheater surface area  $A_1$ , and the appropriate temperature difference:

$$Q = M_r C'_{p1} (t_1 - t_2) = h_2 D_2 L_{vc1} = U_1 A_1 (LMTD)_1$$
(A1.17)

$$A_1 = \frac{M_r C'_{p1} (t_1 - t_2)}{U_1 (LMTD)_1}$$
 (A1.18)

$$h_1 = \frac{C'_{p1} (t_1 - t_2) L_{\nu 1}}{C_{nl} (T_0 - T_1) L_{\nu c1}}$$
 (A1.19)

The logarithmic mean temperature difference  $(LMTD)_1$  is defined as

$$LMTD_{1} = \frac{(T_{c} - t_{2}) - (T_{c} - t_{1})}{\ln(T_{c} - t_{2}) / (T_{c} - t_{1})} = \frac{t_{1} - t_{2}}{\ln(T_{c} - t_{2}) / (T_{c} - t_{1})}$$
(A1.20)

Combining Eqs. (19) and (20) yields

$$\ln \frac{T_c - t_2}{T_c - t_1} = \frac{U_1 A_1}{M_r \bar{C}_{p1}}$$
 (A1.21)

01

$$\frac{T_c - t_2}{T_c - t_1} = e \frac{U_1 A_1}{M_r \bar{C}_{n1}} = e^{NTU_1}$$
 (A1.22)

where NTU is the number of transfer units and is equal to  $(U_1A_1)/(M_r\overline{C}_{p1})$ . The outlet temperature of brine flowing inside the preheater tubes  $t_1$  is given by

$$t_1 = T_c - (T_c - t_2) \overline{e}^{NTU_1} \tag{A1.23}$$

The overall heat transfer coefficient based on the outside surface area is defined by the well known formula

$$\frac{1}{U_0} = \frac{1}{h_i \left(\frac{d_i}{d_o}\right)} + \frac{1}{h_o} + r_i + r_{fi} + r_{fo}$$
(A1.24)

The inside tube heat transfer coefficient can be calculated from Dittus-Boelter equation

$$\overline{Nu} = \frac{h_i d_i}{K_1} = 0.023 Re^{0.8} Pr^{0.4}$$
 (A1.25)

The heat transfer coefficient value is given by

$$h_o = 0.72 g \left[ \frac{g d_L^2 K_1^3 \overline{L}_v}{N m_1 (T_c - T_{su}) d_o} \right]^{1/4}$$
 (A1.26)

where  $\overline{L}_{v}$  is the corrected latent heat of evaporation and is taken as

$$\overline{L}_{v} = L_{v} \left\{ 1 + 0.68C_{p} \left[ T_{c} - 0.5 \left( t_{1} + t_{2} \right) \right] \right\}$$
 (A1.27)

The number of tubes in vertical direction N is related to the shell diameter and pitch by this relation:

$$N = \frac{D_s}{\sqrt{2}P_t} \tag{A1.28}$$

or

$$N = 0.564 \sqrt{N_t}$$
 (A1.29)

For tubes arranged in an equilateral triangular pitch arrangement, the equivalent number of tubes in a vertical row, N, can be predicted from the equation

$$N = 0.481 \left( N_t \right)^{0.505} \tag{A1.30}$$

The total number of tubes  $N_i$  in the brine preheaters is calculated from this relationship:

$$N_{t} = \frac{M_{r}C'_{p1}(t_{1}-t_{2})}{U_{0}pd_{o}L(LMTD)_{1}} = \frac{4M_{r}}{pd_{i}^{2}d_{1}V}$$
(A1.31)

The main differences between the first stage, stage number 1, and any other stage in the heat recovery section, i.e., stage number (Z) are: (1) The brine flow rate to the first stage is  $M_{\rm p}$ 

while it is 
$$\left(M_r - \sum_{1}^{z+1} D\right)$$
 for stage number  $Z$ ;

(2) There is no distillate water flow to the first stage, while for stage number Z it is the accumulated mass of vapors formed in stages

numbers 1 to (Z-1),  $\sum_{1}^{z-1} D$ . Taking these factors

into consideration and following the same procedure discussed in the previous sections, the following equations can be developed for stage number Z in the heat recovery section.

The mass of vapor formed by flashing of brine:

$$D_{z} = \left( M_{r} - \sum_{1}^{z-1} D \right) C p_{z} \frac{T_{z-1} - T_{z}}{L v_{z}}$$
 (A1.32)

The temperature of unevaporated brine flowing from the stage:

$$T_z = Tv_z + BPE_z + NEA_z \tag{A1.33}$$

The concentration of the salt in the stage:

$$S_z = \frac{M_r S_0}{\left(M_r - \sum_{1}^{z} D\right)} \tag{A1.34}$$

The thermal efficiency of the stage:

$$h_{z} = \frac{M_{r}C'p_{z}(t_{z}-t_{z-1})}{(D_{z}=d_{z})L\nu_{cz}}$$
 (A1.35)

The mass of vapor formed due to flashing of distillate flowing from stage number (z-1) to stage number z:

$$d_{z} = \frac{\left(\sum_{1}^{z-1} D\right) C'' p_{z} \left(T c_{z-1} - T c_{z}\right)}{L_{vcz}}$$
 (A1.36)

The heat transfer surface area:

$$A_{z} = \frac{M_{r}C'_{p}(t_{z}-t_{z-1})}{U_{z}(LMTD)_{z}}$$
 (A1.37)

The logarithmic mean temperature difference:

$$(LMTD)_z = \frac{t_z - t_{z-1}}{\ln\left[\left(T_{cz} - t_{z-1}\right)/\left(T_{cz} - t_z\right)\right]}$$
 (A1.38)

The outlet temperature of brine flowing inside the preheater tubes:

$$t_z = T_{cz} - e^{-NTU_z} (T_{cz} - t_{z-1})$$
 (A1.39)

Number of tubes in the preheater:

$$N_{z} = \frac{M_{r}C'p_{z}(t_{z}-t_{z-1})}{U_{z}pd_{o}L(LMTD)_{z}} = \frac{4M_{r}}{pd_{i}^{2}\delta_{1}V}$$
(A1.40)

The developed equations above, which are applied for any stage in the heat recovery section, can also be used for any stage (stage number k) in heat rejection.

Heat transfer surface area:

$$A_{k} = \frac{(M_{f} + M_{c})C'_{pk}(t_{k} - t_{k-1})}{U_{k}(LMTD)_{k}}$$
(A1.41)

The number of transfer units:

$$(NTU)_k = \frac{U_k A_k}{M_f + M_c} \tag{A1.42}$$

The stage thermal efficiency:

$$h_{k} = \frac{\left(M_{c} + M_{f}\right)C'_{pk}\left(t_{k} - t_{k-1}\right)}{\left(D_{k} = d_{k}\right)LVC_{k}}$$
(A1.43)

The total number of tubes in the preheater:

$$N_{t} = \frac{4(M_{f} + M_{c})}{p d_{ik}^{2} d_{2} V_{k}}$$
 (A1.44)

The heat balance on the preheaters of the heat

rejection section gives

$$M_{c} = \frac{\sum_{n-j}^{n} h_{k} (D_{k} + d_{k}) L v c_{k}}{C'_{p} (t_{n-j} - t_{c})} - M_{f}$$
 (A1.45)

The mass and salt balances for the last stage, stage number n, gives

$$S_r = S_b - \frac{M_f}{M_r} (S_b - S_f)$$
 (A1.46)

From the overall mass balance around the plant we get

$$M_f = M_d + M_b \tag{A1.47}$$

For salt mass balance

$$M_f S_f = M_d S_d + M_b S_b \tag{A1.48}$$

Assuming that, the distillate water is free from salt or  $S_d$  is equal to zero yields

$$M_d = \left(\frac{S_b - S_f}{S_b}\right) M_f \tag{A1.49}$$

and

$$M_b = \frac{S_f}{S_b} M_f \tag{A1.50}$$

$$\eta_h M_s L_{vs} = M_r C'_{p1} (T_0 - t_1) \tag{A1.51}$$

$$T_0 - t_1 = \Delta T_{s1} + BPE_1 + NEA_1 + DT_{d1} + TTD_1$$
(A1.52)

The thermal performance, *PR*, of the MSF plant is defined as the mass of distillate water produced per unit mass of heating steam used. That is:

$$PR = \frac{M_d}{M_a}$$

The mass of product distillate water produced  $M_d$  can be related to the mass of recirculated brine by the following equation:

$$M_d = \sum_{i=1}^{n} \left( M_r - \sum_{i=1}^{n-1} D_i \right) Cp_i \frac{T_{i-1} - T_i}{Lv_i}$$
 (A1.54)

Substituting equations and in equation produces

$$PR = \frac{h_{h}Lv_{s} \left[ \sum_{1}^{n} \left( M_{r} - \sum_{1}^{n-1} D_{i} \right) C_{pi} \left( \frac{T_{i-1} - T_{i}}{Lv_{i}} \right) \right]}{M_{r}C'_{p1} \left( \Delta T_{s1} + BPE_{1} + NEA_{1} + \Delta T_{d1} + TTD_{1} \right)}$$
(A1.55)

The heat transfer surface area of the brine heater  $A_h$  is calculated from the following relationship:

$$A_{h} = \frac{M_{r}C'_{p1}(T_{0} - t_{1})}{U_{h}(LMTD)_{h}} = N_{t}pd_{o}L = \frac{pD_{i}^{2}}{4}N_{T}V$$
(A1.56)

The logarithmic mean temperature of the brine heater is given as

$$(LMTD)_h = \frac{T_0 - t_1}{\ln \left[ \left( T_s - T_0 \right) / \left( T_s - t_1 \right) \right]}$$
 (A1.57)

where

$$t_1 = T_s - (T_s - T_0)e^{-(NTU)_h}$$
 (A1.58)

and

$$T_{s} = \frac{\left(T_{0} - t_{1} e^{(NTU)_{h}}\right)}{\left(1 - e^{NTU)_{h}}\right)}$$
 (A1.59)

$$A_s = \frac{\sum_{1}^{n-j} A_i + \sum_{n-j}^{n} A_i + A_h}{M_A}$$

where  $\sum_{i=1}^{n-j} A_{i}$ ,  $\sum_{i=1}^{n} A_{i}$  and  $A_{h}$  are the total heat trans-

fer area in the heat recovery, rejection sections and the brine heater, respectively.

Calculation of the thermal and physical properties of water and water vapor

1. Vapor pressure of saturated water

$$P_v = 23.487 - 0.15T + 2.41 \times 10^{-4}T^2$$

where  $P_{\nu}$ =vapor pressure of saturated water, bar, and T=saturation temperature,  ${}^{\circ}K$ .

2. Saturation temperature

$$T = 307.21 + 127.8 P_{\nu} - 64.1275 P_{\nu}^{2}$$

where T=saturation temperature,  ${}^{\circ}K$ , and  $P_{\nu}$ =saturation vapor pressure, bar.

3. Specific volume of water vapor

$$V_{g} = 1248.643 - 1.91T + 3.651 \times 10^{-3}T^{2}$$

where  $V_g$  = specific volume of water vapor, m<sup>3</sup>/Kg, and T = temperature, K.

4. Specific volume of water

$$V_1 = 5611.453 - 46.436 \ T + 0.1284 \ T^2 - 1.185 \times 10^{-4} T^3$$

where  $V_1$ =specific volume of liquid, m<sup>3</sup>/Kg, and T=temperature,  $^{\circ}$ K.

# 5. Latent heat of evaporation

$$L_{y} = 2589.583 + 0.9156T - 4.8343 \times 10^{-3}T^{2}$$

where L<sub>v</sub>=latent heat of evaporation, kJ/kg.

# 6. Dynamic viscosity of water

$$\mu = 1.278 \times 10^{-3} - 1.835 \times 10^{-5} T + 8.69 \times 10^{-8} T^{-3}$$

where  $\mu$ =water viscosity, Kg/m.s, and T= temperature, K.

## 7. Prandtl number of water

$$P_r = 8.567 - 0.1296T + 6.217 \times 10^{-4}T^2$$

where *Pr*=water Prandtl number and *T*=temp-erature.

Eqs. (A.1)–(A.7) are obtained by correlating the tabulated values of the physical properties. The equations are valid for a temperature range of 300–400°K.

# 8. Specific heat of water at constant pressure

$$C_p = [A + BT + CT^2 + DT^3] \times 10^{-3}$$

# where

 $T = \text{Temperature, } ^{\circ}\text{C}$ 

S = Water salinity, g/Kg

 $A = 4206.8 - 6.6197S + 1.2288 \times 10^{-2} S^2$ 

 $B = -1.1262 + 5.4178 \times 10^{-2} S - 2.2719 \times 10^{-4} S^{2}$ 

 $C = 1.2026 \times 10^{-2} - 5.3566 \times 10^{-4} \text{S} + 1.8906 \times 10^{-6} \text{S}^2$ 

 $D = 6.87774 \times 10^{-7} + 1.517 \times 10^{-6} S - 4.4268 \times 10^{-9} S^{2}$ 

## Appendix 2

Algorithm 1: Brine flowing through the preheater of the i-th stage

$$L_{\nu}(T_{\nu i}) \Rightarrow L_{\nu i}, \quad C_{p}(t_{i}, S_{o}) \Rightarrow c_{pi}$$

$$\frac{L_{vi}D_i\eta}{c_{vi}M_{ro}} \Rightarrow \Delta t_i; (t_i + t_{i+1})/2 \Rightarrow T_{su}$$

$$t_i - \Delta t_i \Rightarrow t_{i+1} \quad P_r(T_{su}) \Rightarrow P_r; \quad \mu(T_{su}) \Rightarrow \mu_i$$

$$\delta_L d_i V / \mu_i \Rightarrow R_e; \quad V = 1.55; \quad \delta_{Li} = 1 / \nu_L (T_{\nu i})$$

0.023 
$$Re^{0.8} P_{ri}^{0.4} K_1 \Rightarrow h_i d_i$$
;  $K_1 = 0.668$ ;  $D_i = 0.01975$ 

$$\begin{split} L_{vi} & \left[ 1 + 0.68 C'_{pi} \left( T_{ci} - T_{su} \right) \right] \Rightarrow L'_{vi}; \quad C'_{pi} = 4.2; \\ T_{su} & = \left( t_i + t_{i+1} \right) / 2 \quad 4 M_{ro} / \left( \pi d_i^2 \delta_{Li} V \right) \Rightarrow N_t \end{split}$$

$$0.564(N_t)^{0.5} \Rightarrow N_r$$
;

$$[N_r] + 1 = N;$$
  $[N_r] = integer part of N_r$ 

$$0.72g \left[ \frac{g \, \delta_{Li}^2 K_1^3 L'_{vi}}{N \mu_i \left( T_{ci} - T_{su} \right) d_o} \right]^{1/4} \Rightarrow h_o; \ g = 9.81$$

$$d_o = 0.03175$$

$$\begin{split} \left[ r_{t} + r_{fi} + r_{fo} + 1/h_{o} + d_{o}/\left(h_{i}d_{i}\right) \right]^{-1} &\Rightarrow U_{i}; \\ r_{t} + r_{fi} + r_{fo} &= 0.000731 \end{split}$$

$$\frac{D_i L_{vi} \eta}{A_o U_i} \Rightarrow LMTD$$

$$t_{i} + \frac{\Delta t_{i}}{\exp\left(\Delta t_{i}/LMTD\right) - 1} \Rightarrow T_{ci}$$

$$D_n/(V_m \delta_{vi}) \Rightarrow a; V_m = 6;$$
  
 $D_n = D_i$  at the last stage  $i = n$ 

$$3.296 \times 10^{-13} L_s \frac{\delta_{Li}}{\delta_{vi}} \left[ \frac{D_i}{a} \right] 2 \Rightarrow \Delta P_{di}; \quad L_s = 0.1;$$

$$\delta_{vi} = 1/v_g (T_{vi})$$

$$\frac{T_{vi}R}{L_{vi}}\ln\left(\frac{P_{vi}}{P_{vi}-\Delta P_{di}}\right) \Rightarrow x; P_{vi}=P(T_{vi})$$

$$R = 0.46152 [kJ/kg (°K)]$$

$$\frac{T_{vi}x}{1+x} \Rightarrow \Delta T_{di}; \quad T_{ci} + \Delta T_{di} \Rightarrow T_{vi}$$

All equations in Algorithm #1 may, formally, be combined in a single non-linear equation and represented by:

$$T_{vi} = g_1 \left( T_{vi,q} \right) \tag{A.1.1}$$

where q is a vector containing all used design values, coefficients and constant values of variables involved in the algorithm and listed above.

It has been verified experimentally that the first derivative

$$d_{g1}(x)/\mathrm{d}x = g'_{1}(x,p)$$

of the function  $g'_1(x,p)$  in the vicinity of the fixed point  $P=T_{vi}$  satisfying (A.1.1) has an approximate value:  $g'_1(P)=0.180$ . Therefore, this fixed point is stable with the following fixed-point iteration:

$$T_{vi}(k+1) = g_1(T_{vi(k),p}), \text{ for } k=0,1,2$$

... up to the condition

$$|T_{\nu i(k+1)} - T_{\nu i(k)}| < \varepsilon = 10^{-5}$$
 (A.1.2)

is satisfied, could be used for calculating the solution of (A.1.1).

Algorithm 2: Brine flowing inside the flashing chamber of the i-th stage

$$C(T_i) \Rightarrow C_i; B(T_i) \Rightarrow B_i$$

$$\sum_{j=1}^{j=i-1} D_j \Rightarrow D_{si}; \quad M_{ro} - D_{si} \Rightarrow M_{ri}$$

$$\frac{M_{ro}S_o}{M_{ri}-D_i} \Rightarrow S_i$$

$$S_i(B_i + C_iS_i) \Rightarrow BPE_i \quad S_i(B_i + C_i) \Rightarrow BPE_i ??$$

105.6 + 18.06 \* 
$$D_{si} \Rightarrow W_i$$
;  
 $D_{si} = \text{sum of } D_i \text{ for } j = [1, i-1]$ 

$$\begin{split} P_{\nu} \big( T_{\nu i} \big) & \Rightarrow P_{\nu i}; \quad P_{\nu} \big( T_{\nu i+1} \big) \Rightarrow P_{\nu i+1}; \\ & 1 / \nu_L \big( T_{\nu i} \big) \Rightarrow \delta_{Li} \end{split}$$

$$P_{vi} - P_{vi+1} - \delta_{Li}(H_i - H_{i+1}) \Rightarrow \Delta P_i$$

 $M_m/W_i \Rightarrow B$ ;  $M_m = M_{ri}$  at the last stage i=n

$$\frac{W_i}{D_d B} \left( 2 \times 10^5 \, \delta_{Li} \Delta P_i \right)^{-1/2} \Rightarrow H_G; \quad C_d = 0.6$$

$$H_G + 0.1 \Rightarrow H_i$$

$$\frac{D_n}{\delta_{vi} V_m 1B} \Rightarrow L_i; \ V_m = 6; \ 1/v_g (T_{vi}) \Rightarrow \delta_{vi}$$

$$a_{T}^{T_{w}}a_{H}^{Hi}a_{W}^{WbW} \Rightarrow NEA_{o}; a_{T}=0.9764;$$
 $a_{H}=15.7378$ 

$$a_w = 1.3777$$
;  $b_w = 3.6 \times 10^{-3}$ 

$$T_{i-1} - T_i \Rightarrow \Delta T_i$$

$$(NEA_o + \Delta T_i/2) \left[ \frac{NEA_o}{NEA_o + \Delta T_i/2} \right] aLLi \Rightarrow NEA_i;$$

$$a_I = 0.3281$$

$$BPE_i + NEA_i + T_{vi} \Rightarrow T_i$$

$$BPE_i + NEA_o + T_{vi} \Rightarrow T_i$$

All equations in Algorithm #2 may, formally, be combined in a single non-linear equation and represented by:

$$T_i = g_2(T_{i,q}) \tag{A.2.1}$$

where q is a vector containing all used design values, coefficients and constant values of variables involved in the algorithm and listed above.

It has been verified experimentally that the first derivative

$$d_{g2}(x)/dx = g'_{2}(x,p)$$

of the function  $g'_2(x,p)$  in the vicinity of the fixed point  $P=T_i$  satisfying (A.2.1) has an approximate

value:  $g'_{2}(P)=-0.082$ .

Therefore, this fixed point is stable and the following fixed-point iteration

$$T_{i(k+1)} = g_2(T_{i(k),p}), \text{ for } k=0,1,2,$$

... up to the condition

$$|T_{i(k+1)} - T_{i(k)}| < \varepsilon = 10^{-5}$$
 (A.2.2)

is satisfied, and could be used for calculating the solution to (A.2.1).

Algorithm 3: Mass of vapor formed in the i-th stage

$$L_{\nu}(T_{\nu i}) \Rightarrow L_{\nu i}; C_{p}(T_{i},S_{i}) \Rightarrow C_{\pi}; \frac{\Delta T_{i}M_{ri}C_{\pi}}{L_{\nu i}} \Rightarrow D_{i}$$

Note that the quantities defining  $D_i$  depend on  $T_{vi}$  and  $T_i$ , and that these variables, as explained in Algorithms #1 and #2, depend on the variable  $D_i$  itself. Therefore, assuming that the fixed point iterations given by (A.1.2) and (A.2.2) have been solved and that the corresponding  $T_{vi}$  and  $T_i$ , satisfying (A.1.3) and (A.2.3), have been calculated, the equations in Algorithm # 3 may, formally, be combined in a single non-linear equation and represented by:

$$D_i = g_3(D_{i,q}) \tag{A.3.1}$$

where q is a vector containing all used design values, coefficients and constant values of variables involved in the algorithm.

It has been verified experimentally that the first derivative

$$d_{g3}(x)/\mathrm{d}x = g'_{3}(x,p)$$

of the function  $g'_3(x,p)$  in the vicinity of the fixed point  $P=D_i$  satisfying (A.3.1) has an approximate value:

$$g_3(P) = -4.4$$
 (A.3.2)

Therefore, this fixed point iteration, if implemented directly using (A.3.1), would be unstable [2]. In order to stabilize the iterative process of calculating the quantity  $D_i$  satisfying (A.3.1), the following modified (stabilizing) equation is considered:

$$D_i = g_3^* (D_{i,q}) = [g_3(D_{i,q}) + (\alpha - 1)D_i]/\alpha$$
 (A.3.3)

which obviously satisfies (A.3.1) for any value of  $\alpha$ , provided that  $\alpha = = 0$ .

Since the first derivative of  $g_3^*(x)$  is given by

$$dg_3^*(x)/dx = g_3^{*'}(x) = \left[g_3'(x) + (\alpha - 1)\right]/\alpha$$

the value of  $\alpha=8$  would make that the function  $g_3^*(x_*p)$  in the vicinity of the fixed point  $P=D_i$  has the value

$$|g_3*'(P)| < 1$$
 (A.3.4)

Thus, the following fixed point iteration

$$D_{i(k+1)} = g_3 * (D_{i(k),p}), \text{ for } k=0,1,2$$

... up to the condition

$$|D_{i(k+1)} - D_{i(k)}| < \varepsilon = 10^{-7}$$

is satisfied, could be used for calculating the solution of (A.3.1) as well as of (A.3.3).